Atmos. Chem. Phys. Discuss., 10, 2669–2710, 2010
www.atmos-chem-phys-discuss.net/10/2669/2010/

Atmospheric Chemistry and Physics Discussions

This discussion paper is/has been under review for the journal Atmospheric Chemistry and Physics (ACP). Please refer to the corresponding final paper in ACP if available.

Assessment of parameterizations of heterogeneous ice nucleation in cloud and climate models

J. A. Curry[1] **and V. I. Khvorostyanov**[2]

[1]School of Earth and Atmospheric Sciences, Georgia Institute of Technology, Atlanta, Georgia, USA
[2]Central Aerological Observatory, Dolgoprudny, Moscow Region, Russian Federation

Received: 16 December 2009 – Accepted: 20 January 2010 – Published: 3 February 2010

Correspondence to: J. A. Curry (curryja@eas.gatech.edu)

Published by Copernicus Publications on behalf of the European Geosciences Union.

Abstract

Several different types of parameterization of heterogeneous ice nucleation for cloud and climate models have been developed over the past decades, ranging from empirically-derived expressions to parameterizations of ice crystal nucleation rates derived from theory (including the parameterization developed by the authors, hereafter referred to as KC). Parameterizations schemes that address the deliquescence-freezing (DF), which combines the thermodynamically indistinguishable modes of condensation freezing and immersion freezing, are assessed here in the context of thermodynamic constraints, laboratory measurements, and recent field measurements. It is shown that empirical schemes depending only on the ice saturation ratio or only on temperature can produce reasonable crystal concentrations, but ice crystal nucleation is thermodynamically prohibited in certain regions of the temperature-saturation ratio phase space. Some recent empirical parameterizations are shown to have insufficient efficiency, yielding clouds that are almost entire liquid at temperatures as low as −35 °C. A reasonable performance of the KC ice nucleation scheme is demonstrated by comparison with data from several recent field campaigns, laboratory data, climatology of cloud phase-state, and GCM parameterizations. Several mis-applications of the KC parameterization that appeared recently in the literature are described and corrected, by emphasizing that a correct application of the KC scheme with simultaneous dependence on the temperature and saturation ratio requires integration of the individual nucleation rates over the measured size spectrum of the environmental aerosol, and not over the spectrum of ice nuclei equal to the crystal concentration at the exit of an experimental device. Simulation with a spectral bin model and correct application of KC scheme adequately describes ice nucleation via the DF mode and yields crystal concentrations and phase state close to those measured in the single-layer stratocumulus cloud observed in the Mixed Phase Arctic Cloud Experiment (MPACE). An assessment of some deficiencies in current parcel modeling methods and cloud chamber observations and their impact on parameterization development and evaluation is provided.

ACPD

10, 2669–2710, 2010

1 Introduction

Ice formation in atmospheric clouds influences the cloud life cycle, precipitation processes, and cloud radiative properties. The importance of cloud ice processes in global climate models has stimulated a large number of theoretical and experimental studies on this topic, but many outstanding problems remain. Further, several recent papers have compared different ice nucleation schemes with contradictory results, raising issues regarding the appropriate application of the schemes, limitations of the parcel model framework, and interpretation of cloud chamber results.

The authors of this paper have developed a theory of heterogeneous ice nucleation (Khvorostyanov and Curry, 2000, 2004a, b, 2005, 2009, hereafter referred to as the KC scheme) that has allowed quantitative description of many features of ice formation in clouds (including simultaneous dependence of the ice nucleation process on both temperature and supersaturation) and created a platform for further improvements of the classical nucleation theory and its practical applications to the parameterization problem. In this paper, we assess the KC nucleation scheme along with several commonly used and recently developed empirical ice nucleation schemes, in the context of thermodynamic constraints and laboratory and field observations. Cloud physics defines the four modes of heterogeneous ice nucleation called sometimes "standard": condensation-freezing, immersion, contact and deposition (Vali, 1985; Pruppacher and Klett, 1997, hereafter PK97). The focus of this assessment is on the deliquescence-freezing (DF) mode, which combines the thermodynamically indistinguishable modes of condensation freezing and immersion freezing.

Over the past several decades, numerous empirical parameterizations have been developed for these four modes of heterogeneous ice nucleation or their combinations, based primarily on laboratory data. Fletcher (1962), Cooper (1986), Sassen (1992), DeMott et al. (1998) suggested parameterizations of ice nuclei (IN) $N_c(T)$ as empirical functions of temperature T. Huffman and Vali (1973), Huffman (1973), and Berezinsky and Stepanov (1986) offered a parameterization consisting of a power law by ice

ACPD
10, 2669–2710, 2010

supersaturation s_i. Meyers et al. (1992, hereafter MDC92) used a continuous flow diffusion chamber (CFDC) to form the basis of an empirical parameterization of the combined condensation-freezing and deposition modes as a supersaturation-dependent only function

$$N_c(s_i) = \exp(a_M + b_M s_i), \quad (1)$$

with N_c in L^{-1}, s_i in %, a_M=−0.639, b_M=0.1296. This parameterization was suggested to be valid at $-20\,^{\circ}C<T<-7\,^{\circ}C$, and 2%<$s_i$<25%, although Eq. (1) has been subsequently applied outside this parameter range. Although the temperature dependence was present in the original data, MDC92 averaged it and included only the supersaturation dependence in the parameterization. A similar s_i-dependent parameterization for deposition nucleation on dust particles was suggested recently by Möhler et al. (2006) based on measurements in a large expansion chamber of 84 m^3.

An empirical parameterization for the immersion mode with soot, mineral dust and biological nuclei was recently suggested by Diehl and Wurzler (2004, hereafter DW04) that generalized Bigg's (1953) concept of the median freezing temperature. This parameterization was tested in the GCM ECHAM4 (Lohmann and Diehl, 2006).

Phillips et al. (2008, hereafter PDA08) developed a new empirical parameterization using MDC92 as a basis. PDA08 extended this parameterization for various T- and s_i-ranges and generalized the parameterization to account for the three types of freezing aerosol (dust and metallic compounds, black carbon, and insoluble organics) by appropriate scaling and integration over the surface areas of these aerosols, so that the concentration $N_{c,x}$ of IN of the x-th kind is

$$N_{c,x} = \int_{\log[0.1\mu m]}^{\infty} (1 - \exp[-\mu_x(D_x, S_i, T)]) \frac{dn_x}{d\log D_x} d\log D_x, \quad (2)$$

where x denotes any of the 3 aerosol types, n_x is the aerosol mixing ratio, and μ_x is the average activated IN per aerosol of diameter D_x; and μ_x is proportional to $N_c(s_i)$ from

Eq. (1) multiplied by some coefficients. For low freezing fraction, which often takes place, $N_{c,x} \sim \mu_x \sim N_c$ (PDA08).

DeMott et al. (2010, hereafter DM10) recently proposed a new parameterization of immersion and condensation freezing as a simple power law function by temperature

$$N_c = a_D(-T_c)^{b_D}(N_{a,05})^{c_D T_c + d_D}, \quad (3)$$

where N_c is in L^{-1}, a_D=1.1968×10^{-5}, b_D=3.6434, c_D=−0.0167, d_D=0.2877, T_c is the temperature in degrees Celsius, and $N_{a,05}$ is the concentration (in cm^{-3}) of aerosol particles larger than 0.5 µm (coefficients may vary a little, see DM10).

Several heterogeneous ice nucleation parameterizations have been suggested based upon theoretical arguments. These parameterizations included analytical fits to the parcel models simulations and various approximations in the basic equations of the crystal growth (e.g., Sassen and Benson, 2000; Lin et al., 2002; Gierens, 2003; Kärcher and Lohmann, 2003; Khvorostyanov and Curry 2005; Liu and Penner, 2005; Barahona and Nenes, 2008, 2009). The use of classical nucleation theory for parameterization of heterogeneous ice nucleation was hampered until recently by the lack of any dependence on supersaturation of the critical radius r_{cr} and energy ΔF_{cr} of ice germs and nucleation rates of freezing process as formulated by J. J. Thomson (1888) (PK97, Eq. 9–38). Khvorostyanov and Curry (2000, 2004a, b, 2005, 2009, hereafter KC00, KC04a, b, KC05, KC09, respectively) extended classical nucleation theory and derived equations for the critical radius and energy that included both T- and S_w-dependencies simultaneously, generalizing the previous expressions derived for homogeneous ice nucleation theory by Khvorostyanov and Sassen (1998, KS98).

The key parameter in classical nucleation theory is the critical radius r_{cr} of an ice germ. The equation for r_{cr} was derived in (KC00) and (KC04a, b) in the form:

$$r_{cr}(T, S_w) = \frac{2\sigma_{is}}{\rho_i L_m^{ef}(T)\left[\ln\left(\frac{T_0}{T}S_w^G\right) - H_{v,fr}\right]}. \quad (4)$$

ACPD
10, 2669–2710, 2010

Here σ_{is} is the surface tension at the ice-solution interface, ρ_i is the ice density, T is the temperature in Kelvin, T_0=273.15, L_m^{ef} is the effective melting heat, S_w is the water saturation ratio, $G = RT/(M_w L_m^{ef})$, M_w is the molecular weight of water, R is the universal gas constant, and a dimensionless function $H_{v,fr}$ describes the effects of the misfit strain ε, finite radius r_a of a haze drop, and external pressure on the drop. The critical energy ΔF_{cr} of a germ formation is (Fletcher, 1969; PK97):

$$\Delta F_{cr}(T, S_w) = \frac{4}{3}\pi\sigma_{is} r_{cr}^2 f(m_{is}, x) - \alpha r_N^2 \sigma_{is}(1 - m_{is}), \quad (5)$$

where m_{is} is the contact or wettability parameter, $x = r_a/r_{cr}$, and α is the relative area of "active sites" (Fletcher, 1969). This becomes with account for Eq. (4) (KC00, KC04a, b)

$$\Delta F_{cr} = \frac{16\pi\sigma_{is}^3 f(m_{is}, x)}{3\left\{\rho_i L_m^{ef}(T)\left[\ln\left(\frac{T_0}{T} S_w^G\right) - H_{v,fr}\right]\right\}^2} - \alpha r_N^2 \sigma_{is}(1 - m_{is}), \quad (6a)$$

which is used in the KC scheme. With $\alpha = 0$ and $H_{y,fr} = 0$, this is simplified (KC00, KC04)

$$\Delta F_{cr} = \frac{16\pi\sigma_{is}^3 f(m_{is}, x)}{3\left[\rho_i L_m^{ef}(T)\ln\left(\frac{T_0}{T}\right) + \frac{\rho_i RT}{M_w}\ln S_w\right]^2}, \quad (6b)$$

The nucleation rates J_{het} in classical nucleation theory are evaluated as (Fletcher, 1962; Dufour and Defay, 1963; PK97; Seinfeld and Pandis, 1998)

$$J_{het} = \frac{kT}{h} N_{mon} Z_s \Omega_s c_{1s} 4\pi r_N^2 \exp\left(-\frac{\Delta F_{act} + \Delta F_{cr}}{kT}\right), \quad (7)$$

where ΔF_{act} is the activation energy, k and h are the Boltzmann's and Planck's constants, c_{1s} is the concentration of water molecules adsorbed on 1 cm^2 of a surface, r_N

is the radius of insoluble substrate, N_{mon} is a number of monomers of water in contact with unit area of ice surface, Ω_s is the surface area of the germ, and Z_s is the Zeldovich (1942) factor refined for heterogeneous nucleation in Vehkamäki et al. (2007).

The total number of particles nucleated in deliquescence-freezing mode (IN concentration) is obtained by integrating over the aerosol size spectrum $f_a(r_a)$:

$$N_c(t) = \int_{r_{min}}^{r_{max}(s_{max})} P_{fr}(r_a, r_N, t) f_a(r_a) dr_a, \quad (8)$$

where $P_{fr}(r_a, r_N, t) = 1 - \exp\left(-\int_0^t J_{het}(r_a, r_N, t')dt'\right)$ is the probability of freezing at a time t of a single deliquescent CCN (haze) particle with radius r_a containing an insoluble substrate with radius r_N. The crystal nucleation rate R_{fr} ($cm^{-3}\,s^{-1}$) in a polydisperse aerosol can be calculated as:

$$R_{fr} = \frac{dN_{fr}}{dt} = \int_{r_{min}}^{r_{max}} dr_N f_a(r_N) J_{s,fr}(t) \exp\left(-\int_0^t J_{s,fr}(t')dt'\right) \quad (9)$$

The system of Eqs. (4–9) comprise the essence of the KC heterogeneous ice nucleation scheme with simultaneous account for the dependence on temperature, humidity, misfit strain, finite size of freezing particles and external pressure that was used in KC00-KC09 to describe critical radii and energies, kinetics, thresholds and other properties of heterogeneous ice nucleation. The input information includes data for individual aerosol particles obtained in experiments: contact angle or wettability parameter, activation energy ΔF_{act}, surface tension. Hence the KC ice nucleation scheme enables determination of aerosol specific properties and differences in their nucleation abilities.

Liu and Penner (2005) used a particular case of ΔF_{cr} from KC00 work, Eq. (6b) with $H_{v,fr}$=0 and α=0, i.e., without account for misfit strain, the finite radius of a haze drop and without active sites (Eq. 2.6 in Liu and Penner) to develop an ice nucleation parameterization for a GCM (Liu et al., 2007). Eidhammer et al. (2009) used more

ACPD
10, 2669–2710, 2010

detailed Eqs. (4) and (6a) for r_{cr} and ΔF_{cr} for a comparison of the KC and PDA08 schemes; this work is analyzed below.

Chen et al. (2008) refined calculations of the nucleation rates in the classical nucleation theory by fitting its parameters (ΔF_{act}, m_{is}) based on laboratory measurements of ice nucleation on IN of various origin (soot, bacteria, pollen, and dust). It was shown in Chen et al. (2008) that the contact parameters of several substances can be very close to unity, which may explain the high temperature threshold of ice nucleation when such substances are present. A deficiency of the Chen et al. (2008) scheme was that the classical theory for freezing was used without S_w-dependence. As Eqs. (4) and (6a) show, this may substantially influence the values of the parameters; in particular, fitted ΔF_{act}, m_{is} in the freezing modes should depend on humidity and have different values at various humidities.

In this paper, we analyze several empirical parameterizations and compare them with the KC theoretical approach based on the classical nucleation theory. In Sect. 2, thermodynamic constraints on heterogeneous ice nucleation are examined. In Sect. 3, an empirical parameterization by Phillips et al. (2008; hereafter PDA08) is compared with the theoretical KC ice scheme in parcel model simulations in evaluation with the climatological data and GCMs parameterizations of cloud phase state. Section 4 compares the results of numerous parcel runs with KC ice nucleation scheme to the results of ice nuclei measurements in the six recent field campaigns and some laboratory measurements. In Sect. 5, the low-level mixed-phase arctic cloud observed during MPACE is simulated using a 1-D model with spectral bin microphysics and it is shown that the KC ice scheme reproduces the correct quasi-state mixed phase of this cloud for a few hours. A brief summary is given in Conclusions.

2 Thermodynamic constraints on heterogeneous ice nucleation schemes

Heterogeneous nucleation schemes that depend on temperature and/or supersaturation have been derived from both empirical and theoretical bases. Here we assess the

ACPD
10, 2669–2710, 2010

range of validity of these parameterizations in the context of thermodynamic constraints derived from the extended classical nucleation theory described by KC.

The critical radius r_{cr} of an ice germ in Eq. (4) is positive if the denominator is positive, yielding a condition for the threshold $S_{w,th}(T)$ or $T_{th}(S_w)$ for ice particle nucleation (KC04a, b, KC09):

$$S_{w,th}(T) = \left(\frac{T}{T_0}\right)^{M_w L_m^{ef}/RT} \exp\left[\frac{M_w}{\rho_i RT}\left(C_\varepsilon \varepsilon^2 + \frac{2\sigma_{sa}}{r_a} + \frac{\Delta\rho\Delta p}{\rho_w}\right)\right], \quad (10)$$

$$T_{th}(S_w) = T_0 S_w^{RT/M_w L_m^{ef}} \exp\left(-\frac{C_\varepsilon \varepsilon^2}{\rho_i L_m^{ef}} - \frac{r_{sc}}{r_a} - \frac{\Delta\rho\Delta p}{\rho_w \rho_i L_m^{ef}}\right). \quad (11)$$

Here σ_{sa} is the surface tension at the solution-air interface, ρ_w is the water density, $C_\varepsilon \sim 1.7\times10^{11}$ dyn cm^{-2} is the Turnbull-Vonnegut parameter (PK97), $\Delta\rho=\rho_w-\rho_i$, $\Delta p=p-p_0$ is the excess pressure, p_0 is the reference pressure (1 atm), p is the external applied pressure, $r_{sc}=2\sigma_{sa}/(\rho_i L_m^{ef})$ is the curvature parameter and the term r_{sc}/r_a describes the effects of curvature of a haze drop on ice nucleation. Equations (10) and (11) represent a lower and upper limiting cases for S_w and T, respectively for an infinitesimally small nucleation rates J_{het}, the more general equations for finite J_{het} are given in KC04b, KC09, they predict somewhat higher $S_{w,th}$ and lower T_{th}.

Equations (4), (10), and (11) show that the value $r_{cr}>0$ if $S_w>S_{w,th}$ at given T or $T<T_{th}$ at given S_w, and only these states are thermodynamically allowed in the S_w–T domain. The denominator of the critical radii r_{cr} of ice germs in Eq. (4) becomes negative and $r_{cr}<0$ in the S_w-T domain if $S_w<S_{w,th}$ at given T or $T>T_{th}$ at given S_w, where relative humidity over water (RHW) is smaller than its threshold value, RHW<RHW$_{th}$ i.e. δ(RHW$_{th}$)= RHW−RHW$_{th}$=($S_w-S_{w,th}$)×100%<0 (see also KC04b, KC09).

Here we assess the range of thermodynamic validity of the MC92, PDA08, and DM10 ice nucleation parameterization schemes on the S_w–T diagrams using values of N_c calculated with parameterizations (Eqs. 1 and 3). Calculations were performed over

ACPD
10, 2669–2710, 2010

the full range of values of s_i and T. For comparison with $S_{w,th}$ and $\delta(RHW_{th})$, these quantities were calculated for pairs of S_i and T values. Calculated $N_c(S_i)$ and $N_c(T)$ were superimposed on the field of $\delta(RHW_{th})$ in Fig. 1 in S_w–T coordinates.

Figure 1 represents an S_w–T diagram, the entire considered domain is $-30\,^{\circ}C < T < 0\,^{\circ}C$ and $0.7 < S_w < 1.0$. Superimposed here is the threshold difference $\delta(RHW_{th})$. The deep blue hatched line denotes the boundary $RHW = RHW_{th}$. Below the hatched line, $r_{cr} > 0$, and these states are thermodynamically allowed. The states above the deep blue hatched line (white field) correspond to the negative values of r_{cr}. That is, ice germs cannot be nucleated above this line in this S_w–T area, which therefore is thermodynamically prohibited. Only the states below the blue hatched line $RHW - RHW_{th} = 0$ (shaded field) are thermodynamically allowed for heterogeneous ice nucleation. Figure 1 shows that this allowed T–S_w domain is located in the triangle below temperature of -8 to $-12\,^{\circ}C$ and at water saturation ratio above 0.8 to 0.83. This area covers only about 1/8 of the entire considered domain. The rest 7/8 of this domain are allowed for ice nucleation in MDC92 and DM10 schemes but are inhibited thermodynamically because the ice germ radii are negative here. The boundaries of the allowed domain depend of the size r_a of aerosol particles. When r_a increases from 0.05 µm, typical of the fine mode, to 1 µm typical of the coarser mode, the allowed domain shifts to higher temperatures, in this example by about $5\,^{\circ}C$.

It is interesting to note that the isolines of MDC92 s_i-parameterization are in good correlation (almost parallel) with the isolines of $\delta(RHW_{th})$ that follow from the generalization of classical theory in KC. This indicates that MDC92 captures some basic features of the nucleation process. However, the gradients dN_c/dS_w and dN_c/dT in MDC92 are noticeably smaller than predicted by the classical theory. The agreement of DM10 parameterization with classical theory is somewhat worse because it does not account for the humidity dependence.

We do not present here similar thermodynamic analysis of the other existing parameterizations but it can be done for any function $N_c(T)$ and $N_c(s_i)$ and should be accounted for when constructing the new parameterizations. These thermodynamic

ACPD
10, 2669–2710, 2010

limitations also should be accounted for when choosing and comparing the empirical and theoretical parameterizations of ice nucleation in the numerical models of various complexity as e.g., in Comstock et al. (2008) and Eidhammer et al. (2009).

3 Evaluation of phase state simulations

Eidhammer et al. (2009; hereafter EDK09) compared three parameterizations of heterogeneous ice nucleation using a parcel model developed at Colorado State University (CSU). The model is based on the spectral bin microphysics for the mixed and ice states with various parameterizations of ice nucleation. The three ice nucleation schemes included PDA08, KC, and DW04. Comparing the results of simulations for the three parameterizations, EDK09 found that for small vertical velocities $w \sim 5\,\mathrm{cm\,s^{-1}}$, all three parameterizations yield similar results. For large w, only PDA08 compares well with typical observations of ice nucleation in CFDC producing $N_c \sim 1\text{–}15\,\mathrm{L^{-1}}$, while the other two parameterizations (DW04 and KC) produce crystal concentrations several orders of magnitude higher than PDA08. EDK09 recommend that the empirically-derived "constraint" on the upper limit of N_c used in the PDA08 scheme should be used in cloud and climate models parameterizations.

In this section, the PDA08 and KC schemes are compared further to understand the sources of the discrepancies between the two parameterizations (we note that the DW04 scheme performs comparably to KC and produces comparable N_c). We perform simulations using the parcel model described in KC05. The drop nucleation was substantially modified according to Khvorostyanov and Curry (2006, 2007, hereafter KC06, KC07), where a generalized power law $N_d(s_w)=C(s_w)s_w^{k(s_w)}$ was derived. Both C and k depend on water supersaturation s_w and decrease with increasing s_w, in agreement with the observed experimentally quantities (Yum and Hudson, 2001), yielding finite N_d limited by N_a at high s_w. We used the same composition of aerosol as in EDK09, and the KC heterogeneous DF ice nucleation scheme. Simulations are conducted with the

active site area α in Eq. (6a) in two forms: α=0; and parameterized as a function of T,

$$\alpha(T) = \alpha_0(1 - T_c/T_v)\theta(T_{th} - T_c)\theta(T_c - T_v), \quad (12)$$

where $\alpha_0 = 2\times10^{-5}$ as tested in KC05, $\theta(x)$ is the Heaviside function, $T_{th} = -5\,^{\circ}$C is the threshold temperature of nucleation close to that assumed in EDK09, and $T_v = -20\,^{\circ}$C is the scaling temperature that determined the rate of decrease in $\alpha(T)$. Equation (12) indicates that $\alpha(T)$ has a maximum $\alpha_0 = 2\times10^{-5}$ at warm T, and decreases to 0 at $T = -20\,^{\circ}$C. This parameterization is intended to account for the fact that the area of the sites close to the structure of water (m_{is}=1) increases toward 0 °C. We hypothesize that these sites can be formed by some crystal defects, steps, or premelted sites or other reasons. Their exact origin does not matter for now, but it is known that the number of such sites may increase toward 0 °C (Hobbs, 1974; Dash et al., 1995).

The results of simulations from EDK09 with ice scheme PDA08 and from our parcel model with the KC scheme and two forms of α are compared in Fig. 2. The initial RHW=89%, and drop activation occurs in a few minutes. The drop concentration N_d is ~90 cm^{-3} in EDK09 model and 160 cm^{-3} in KC model, the difference associated with different drop activation methods. Values of N_d are constant in EDK09 simulations for 4 h (Fig. 2c), and liquid water content (LWC) increases over this period due to drop growth down to $T = -34.5\,^{\circ}$C (Fig. 2e). In the EDK09 model, noticeable heterogeneous crystal nucleation begins at about 75 min when $T < -3\,^{\circ}$C, their concentration N_c increases almost linearly and reaches ~22 L^{-1} at $T \sim -32.5\,^{\circ}$C at a height above 6 km and time 240 min (Fig. 2d). Thus, nucleation with PDA08 scheme continues over almost 4 h, much longer than in any other heterogeneous scheme (e.g., Sassen and Benson, 2000; Lin et al., 2002; Kärcher and Lohmann, 2003; KC05; Liu and Penner, 2005). Then an abrupt increase in N_c occurs by almost 3 orders of magnitude to 1.6×10^4 L^{-1} that is apparently caused by turning on homogeneous nucleation, which is allowed in EDK09 model at the heights above 6 km, i.e., at $T \approx -34\,^{\circ}$C. At temperatures warmer than −34 °C, the nucleated ice crystals do not influence N_d and LWC, and no signs of Bergeron-Findeisen process and crystallization kinetics are seen on

ACPD
10, 2669–2710, 2010

the EDK09 curves. Only when the temperature falls to −34.5 °C and N_c increases almost by three orders of magnitude due to homogeneous nucleation, both N_d and LWC abruptly drop to zero, apparently due to instantaneous crystallization by the crystals homogeneously formed at T=−34 to −35 °C. Thus, the crystals heterogeneously formed in PDA08 scheme are unable to produce any noticeable crystallization effect and the "constraints" imposed in the PDA08 scheme lead to a substantial underestimation of heterogeneous ice nucleation.

In contrast, crystallization in the KC scheme occurs much more smoothly with decreasing temperature, in the temperature range of ∼15 °C. With α=0, crystal nucleation in KC scheme begins at −15 °C and N_c reaches a maximum $\sim 10^3$ L^{-1} within 2 °C. With the smooth value of $\alpha(T)$, crystal nucleation begins at about −5°C, and ends at −17 °C, much more smoothly than with α=0. N_d and LWC begin to decrease at −20 °C with α=0 (at −10 °C with $\alpha(T)$) and vanishes at −35 °C with α=0 (at −23 °C with $\alpha(T)$), within 1 h in both cases. The DW04 scheme (Fig. 1 in EDK09) is not shown here, but it performs similarly to the KC scheme, and produces realistic crystallization and cloud phase state.

The phase state in clouds is characterized by the ratio of the liquid (LWC) to the total water (LWC+IWC) in mixed phase, f_l =LWC/(LWC+IWC)×100%. Figure 3 shows the observed climatology of f_l compiled of a few thousands aircraft measurements (Borovikov et al., 1963; reproduced in PK97). In pure liquid clouds at warm temperatures slightly below 0 °C, f_l is close to 100%, then decreases with decreasing temperature (22% liquid at −15 °C) and tends to zero at T<−30 °C, i.e., the clouds become purely crystalline. Figure 3 compares this climatological data with f_l calculated from the simulation data of EDK09 and from KC scheme (shown in Fig. 2 above) with two forms of $\alpha(T)$. These are also compared with the two parameterizations of f_l as a function of temperature in two general circulation models: ECMWF (European Centre for Medium-Range Weather Forecasts) and NCAR CAM3 (National Center for Atmospheric Research Community Atmosphere Model 3). In ECMWF, it was chosen as $f_l=[(T-T_{ice})/(T_0-T_{ice})]^2$, and f_l=0 at $T<T_{ice}$, with T_0=273.16 and T_{ice}=250.16 K (12% liq-

ACPD
10, 2669–2710, 2010

uid at −15 °C), (ECMWF-2007). In NCAR CAM3, the ice fraction was parameterized as $f_i(T)=(T-T_{max})/(T_{min}-T_{max})$ with $T_{max}=-10$ °C, $T_{min}=-40$ °C (Boville et al., 2006); then f_l in percent can be written as $f_l(T)=1-f_i(T)=(T_{min}-T)/(T_{min}-T_{max})\times 100$, and $f_l(T)=0$ at $T<T_{min}$ (83% liquid at −15 °C). Figure 3 shows that the ECMWF parameterization is very close to the climatological data by Borovikov et al. (1963), but ends at a little warmer temperatures. The CAM3 parameterization has a slope close to the climatological data, but the curve CAM3 is displaced as a whole toward colder temperatures by about 10 °C, underestimating the ice phase at warm and medium temperatures (note that the T-limits in NCAR CAM2 were 0 and −20 °C (Boville, 2006), and $f_l(T)$ was closer to the ECMWF).

The $f_i(T)$ slopes in the KC scheme are steeper than the climatological, ECMWF and CAM3 values but are still comparable with them, and closer to CAM3. Occurrence of the ice phase increases in KC scheme at −16 °C with $\alpha=0$ and at −10 °C with $\alpha(T)$; the threshold with $\alpha(T)$ is close to the threshold in CAM3. In general, the KC scheme may underestimate ice phase at warm temperatures and overestimate the ice phase at cold T. However, there is a clear qualitative agreement of the KC scheme with the climatological data and parameterizations ECMWF and CAM3, although a smoothing of the KC curve over the wider T-range is desirable, which is discussed below.

In contrast, the EDK09 data based on the PDA08 parameterization are in sharp conflict with climatology, ECMWF and CAM3. EDK09 predicts more than 95% of liquid phase down to −34.5 °C, where homogeneous nucleation begins to act. We note that the threshold value of −34.5 °C for homogeneous nucleation chosen in EDK09 is 4–6 °C warmer than it should be, −38 to −40 °C (e.g. PK97). With homogeneous nucleation, the PDA08 curve exhibits abrupt crystallization within a few tenths of a degree, and the curve $f_l(T)$ is actually vertical. The simulations in EDK09 show that the DW04 scheme produces ice crystals with concentrations similar to the KC scheme, i.e., with the limits 300 L^{-1} for dust and 1000 L^{-1} for soot, the corresponding limiting aerosol concentrations in the 2nd mode chosen in EDK09.

The low heterogeneous nucleation efficiency of the PDA08 scheme in ice production

was somewhat masked in Fig. 2, where the characteristics of the liquid and ice phases were plotted separately, but it becomes clearer in Fig. 3, when considering the ratios of liquid to total water, i.e., $f_l(T)$. Figure 3 illustrates that the increase in LWC during the parcel ascent is so rapid that the small amount of ice nucleated did not result in any noticeable crystal growth and liquid water depletion by the Bergeron-Findeisen mechanism. EDK09 argued that the KC and DW04 schemes produced crystal concentrations a few orders of magnitude greater and substantially overestimate ice production. However, Fig. 3 shows that the KC scheme is much closer to reality (and the DW04 scheme also), while the PDA08 scheme produces unrealistically high values of liquid water down to the imposed threshold of homogeneous nucleation.

4 Assessment of parameterized ice particle concentrations

Phillips et al. (2008) and EDK09 compared the PDA08 empirical parameterization of IN with that from KC theory and concluded that the KC approach produces $N_c(T)$ curves with slopes dN_c/dT that are too large and overestimate the crystal concentration N_c. In this section, we show that PDA08 used an incorrect procedure of comparison, and a correct comparison shows good agreement of the KC heterogeneous DF ice nucleation scheme with observations.

Figure 4 shows the results of simulations of N_c with the parcel model described in KC05 and KC heterogeneous DF ice nucleation scheme. This figure includes simulations from KC05 based on several hundred runs of the parcel model, and results of several new runs are added along with our parameterizations for w=0.3 to 50 cm s^{-1} and Cooper's (1986) parameterization. Each solid symbol in Fig. 4 corresponds to a final value of N_c after a single run of the parcel model with the KC scheme. This figure shows substantial variability of N_c that depends on the initial temperature T, vertical velocity w, contact parameter m_{is}, and the area α of the active sites. The KC curves of $N_c(T)$ have two distinct different slopes: a larger slope at $T<-18$ to -20°C and a smaller slope for $T<-20$°C. The two different slopes are explained by the preferen-

ACPD
10, 2669–2710, 2010

tial ice nucleation with medium contact parameter m_{is}~0.5 in mixed phase clouds at $T > -20\,^{\circ}C$ (red symbols) and in ice clouds at colder temperatures (blue symbols). However, mixed-phase clouds may exist in these simulations down to $-30\,^{\circ}C$ at lower values of m_{is}, which indicates that the KC scheme can be consistent with frequent observations of the mixed-phase Arctic clouds at low temperatures (Curry, 1986; Curry et al., 1990, 1993, 1996, 2000; Gultepe et al., 2000; Lawson et al., 2001; Intrieri et al. 2002; Korolev et al., 2003; Shupe et al., 2006; McFarquhar et al., 2007). A comparison with Cooper's (1986) parameterization limited at $N_c = 500\,L^{-1}$ shows that the slopes of the KC curves are greater at $T > -18\,^{\circ}C$ and much smaller at colder T in mostly crystalline clouds.

The solid lines with the open symbols in Fig. 4 represent a parameterization of the simulation data described in KC05 and modified here as a function of two variables, T and w:

$$N_c(T,w) = C_g(T_{c0} - T_c)^{C_T} w^{C_w}, \tag{13}$$

where T_c is the temperature in Celsius, $T_{c0} = 0\,^{\circ}C$, N_c is in L^{-1}, $C_w = 1.41$; and there are two sets of the other constants: $C_g = 0.4 \times 10^{-8}$, $C_T = 8.0$, for $T_c > -15\,^{\circ}C$; and $C_g = 0.535$, $C_T = 1.05$ for $T_c < -15\,^{\circ}C$. The expression in Eq. (13) represents the average data in Fig. 4 and can be used as a simple parameterization in cloud models and GCMs.

This parameterization (13) is compared in Fig. 5 to the experimental data from the 6 field campaigns described in EDK09: INSPECT1, INSPECT2, CRYSTAL-FACE, PACDEX, WISP, and MPACE. Figure 5 shows that the span of the KC parameterization curves in the range $w = 0.3$–$5\,cm\,s^{-1}$ encloses the majority of the field data, i.e., this ice nucleation scheme is in general agreement with the field experiments. The tendency of KC curves is in a qualitative agreement with Copper's (1986) parameterization used in the Morrison microphysics scheme current employed in the CAM3 GCM (Morrison and Gettelman, 2008; Gettelman et al., 2008) but allows a greater variability caused by the different cooling rates (w). The almost vertical curve in Fig. 5, marked "PDA-KC", is from PDA08. This curve was labeled "KC" in PDA08 and was intended

to represent the T-dependence in KC theory. However, Figs. 4 and 5 clearly illustrate that this "KC" curve in PDA08 does not correspond to the KC scheme and does not represent any real dependence of final $N_c(T)$ from KC simulation data for various conditions. This curve is completely different from the real T-dependences in KC scheme shown in Figs. 4 and 5; it was constructed in PDA08 for the first time without any parcel simulations and therefore is named here "PDA-KC". It differs from the KC simulations here in two aspects: 1) the slope of this curve is much steeper than that of the KC curves; 2) the maximum values of $N_c(\sim 2\times 10^5\,\mathrm{L}^{-1})$ are 10^3–10^5 times greater than on the KC curves. These differences are analyzed below.

The PDA-KC curve is almost vertical because ice nucleation in this case occurs in a very narrow T-range, in this case, $\sim -14\,^{\circ}\mathrm{C}$ to $-16\,^{\circ}\mathrm{C}$. This curve was plotted in PDA08 as a possible hypothetical temperature dependence of intermediate $N_c(T)$, but it was calculated without any parcel model runs, simply from Eq. (8) with fixed S_w=1 (or RHW=100%); that is, with excluded S_w-dependence. This curve actually represents the old T-dependence based on the classical equations for r_{cr} and ΔF_{cr} by J. J. Thomson (1888) with account for only the T-dependence and without the S_w-dependence (see PK97, Eq. 9–38). It has long been known that early formulations of the classical nucleation theory produce unrealistic values of N_c. PDA08 characterized this curve as a T-dependence in the KC scheme, but it is an incorrect characterization because the T-dependence in the KC parcel model simulations shown in Figs. 4 and 5 corresponds to many nucleation events that begin at different initial conditions (T, S_w) and pass different trajectories on the $S_w - T$ phase plane, and the temperature in KC data is the final temperature when nucleation has ceased. The very large values of N_c that are 3–5 orders of magnitude higher than typical N_c were produced by PDA08 using only Eq. (8) for N_c and fixing S_w=1, and therefore neglecting very strong negative supersaturation feedback in the KC scheme (see KC05). If the correct S_w-dependence is included, then S_w becomes negative at some N_c, and creates an exponential negative feedback and nucleation ceases at values of N_c represented by KC points in Fig. 4 and curves in Fig. 5 that are 3–5 orders of magnitude smaller than those on the "PDA-KC" curve.

ACPD
10, 2669–2710, 2010

Therefore the PDA08 interpretation of the KC theory with excluded S_w-dependence is an incorrect representation of the KC parameterization. The strong negative feedback due to S_w-dependence found and analyzed in KC05 bounds N_c and produces much smoother $N_c(T)$ and parameterization that are in a good general agreement with the data from 6 field campaigns as shown in Fig. 5.

Figure 6 shows another comparison of $N_c(s_i)$ calculated with KC scheme with experimental data by Rogers (1982, 1988) and Al Naimi and Saunders (1985), now as a function of ice supersaturation. Plotted here are also two previous empirical parameterizations, MDC92 (green) and Huffman's (1973) power law $N_c(s_i)=C_{iH}s_i^{b_H}$ (magenta). Huffman found $3<b_H<8$, and C_{iH} was more uncertain. We have chosen here the values $C_{iH}=10^{-5}\,L^{-1}$ and $b_H=4.9$ to match the lab data. Each solid symbol on the theoretical curves or nearby (red, blue and brown) corresponds to a final N_c (after nucleation ceases) in a single run of the parcel model plotted against the maximum value of s_i during the run (reached usually near maximum N_c). The points from parcel simulations with KC scheme are here the same as in Fig. 4 for $N_c(T)$ but plotted now versus s_i.

Figure 6 shows that KC values of N_c are in reasonable qualitative and quantitative agreement with the experimental points and both previous parameterizations, showing an increase of $N_c(s_i)$ with increasing s_i. However, the simulated increase is different for both small and large values of s_i: there is a distinct decrease of the slopes $dN_c(s_i)/ds_i$ at $s_i>15$–20%, i.e., some sort of "saturation" at higher s_i. This feature, convex dependence $N_c(s_i)$ with decreasing slopes, is similar to Huffman's parameterization and to the water supersaturation dependence in the drop nucleation power law (e.g., Yum and Hudson 2001).

5 Simulations of Mixed-Phase Arctic Cloud Experiment (MPACE)

One of the greatest challenges for a heterogeneous ice nucleation parameterization is in the simulation of the long-lived mixed phase clouds that occur in the Arctic. The Mixed-Phase Arctic Cloud Experiment (MPACE) was conducted during September-

ACPD
10, 2669–2710, 2010

October 2004 at the North Slope of Alaska site in the vicinity of the ARM Climate Research Facility (Verlinde et al., 2007). A single-layer mixed-phase stratocumulus cloud deck with the boundaries from 0.4–0.5 to 1.3–1.6 km was observed on 9–11 October, when the air mass was advected from the pack ice to the open ocean and further inland (Klein et al., 2006; Verlinde et al., 2007). The temperature varied from approximately around −8 °C at cloud base to −15 to −17 °C at cloud top (McFarquhar et al., 2007). The data on condensation nuclei were absent due to instrument malfunction onboard of Citation aircraft. The dry aerosol size distributions were obtained with Hand-Held Particle Counter (HHPC) on the Aerosonde unmanned aircraft, but aerosol composition was unknown, and some condensation nuclei data were collected by the counter operated in Barrow.

The average aerosol measurements on 10 October were approximated by a bimodal aerosol size spectrum that was recommended for use in numerical models (Klein et al., 2006). The parameters for the fine mode were: concentration N_{a1}=72.2 cm^{-3}, mean geometric radius r_{g1}=0.052 µm, and dispersion σ_{d1}=2.04; the corresponding parameters for the coarse mode were N_{a2}=1.8 cm^{-3}, mean geometric radius r_{g2}=1.3 µm, and dispersion σ_{d1}=2.5.

The data on IN were sampled onboard of Citation with a CFDC having an upper radius limit of 0.75 µm. 96% of the data remained below the CFDC detection limit of about 0.1 L^{-1}, although measured crystal concentrations varied in the range 1–30 L^{-1} (Fridlind et al., 2007). We can hypothesize two possible reasons of this. One reason could be that the CFDC radius limit, 0.75 µm, was substantially lower than the mean radius of the second aerosol mode, 1.3 µm. Thus, the IN particles in the tail of the 2nd aerosol mode with maximum surface area and potentially highest ice nucleability were excluded from CFDC measurements, while the concentration of large particles only 0.01 cm^{-3}=10 L^{-1} would produce a significant effect. An additional explanation could be that the time of IN processing in the CFD chamber, 7–15 s (Rogers, 1982, 1988; PDA08), is much smaller than the timescale of heterogeneous ice nucleation of 15–240 min determined from models (e.g., Lin et al., 2002; KC05; EDK09). So, the

ACPD
10, 2669–2710, 2010

IN concentrations above detection limit were measured only during 4% of the in flight measurement time, when IN concentration reached 1–20 L^{-1}. Published simulations of this case used the average value of 0.16–0.2 L^{-1}, which was determined as the average of 0 (below the detection limit) and the highest values of IN (Prenni et al., 2007, Fridlind et al. 2007; Morrison et al. 2008).

Several simulations of MPACE were performed with various models and ice nucleation parameterizations. Prenni et al. (2007; hereafter P07) used the Regional Atmospheric Modeling System (RAMS, Cotton et al., 2003) with heterogeneous ice nucleation parameterized using MDC92 and its modification with the same the functional form as Eq. (1) but with different coefficients a_M=−1.488, b_M=0.0187. P07 found that simulations with MDC92 led to rapid cloud glaciation even with depletion of IN, lack of liquid water and small optical thickness. Simulations with the modified MDC92 scheme (P07 ice scheme) and depletion of IN produced a mixed-phase cloud deck with sufficient liquid phase similar to observations. Simulations with the P07 scheme and IN increased by a factor of 2 and 10 (to ∼0.4–2 L^{-1}) still yielded a mixed cloud and liquid phase was maintained for 24–48 h. However, simulations using the P07 scheme without IN depletion led again to rapid glaciation.

Fridlind et al. (2007) simulated the MPACE cloud using a 3-D LES model with sized-resolved bin microphysics. Several pathways of ice nucleation were parameterized in the model including the four standard modes of pristine ice nucleation, various modes of ice multiplication, and a few additional mechanisms. These mechanisms included: increase of IN aloft by 3 orders from 0.2 to 200 L^{-1}, surface source of IN, prescription of some arbitrary rates of volume and surface freezing, slower sedimentation plus fragmentation, ice nuclei formation from drop evaporation residues, and drop freezing during evaporation. Fridlind et al. (2007) found that the ambient IN as measured by CFDC appeared insufficient by several orders of magnitude to explain observed cloud phase state, in particular, crystal concentrations and IWC. Sensitivity tests showed that neither standard 4 heterogeneous ice nucleation modes, nor 2 common ice multiplication mechanisms (drop shattering and crystal fragmentation due to ice-ice collisions)

ACPD
10, 2669–2710, 2010

could explain the observed cloud microstructure and phase state. The standard modes and even increase of IN by 3 orders aloft (run 200/L) could produce only N_c generally smaller than 1–2 L^{-1}. The runs with either evaporation freezing or with evaporation IN produced total crystal concentrations of 10 L^{-1} and greater. This however did not cause full cloud glaciation and vertical profiles of LWC were similar to observed values with maxima about 0.5 g m^{-3} at a height 1200 m. Both LWP and IWP were also similar to observed values in these runs.

Morrison et al. (2008) simulated MPACE using the polar version of mesoscale MM5 model with two-moment microphysics scheme (Morrison et al., 2005; Morrison and Pinto, 2005). Two different modes of ice nucleation were included: deposition, condensation-freezing and immersion-freezing were considered as a single mode with a specified value of IN concentration of 0.16 L^{-1}; and contact nucleation was parameterized with the temperature dependence following MDC92. The model was able to reproduce the LWC and drop concentrations in reasonable agreement with observations but could not capture ice phase properties as well. The modeled crystal concentration was smaller than observed by about an order of magnitude, which was a consequence of the large discrepancy between the measured IN and ice crystal concentrations. The sensitivity to ice nuclei concentration was tested by increasing IN by 10 and 100 times in the runs IN×10 (to 1.6 L^{-1}) and IN×100 (to 16 L^{-1}). The run IN×10 produced crystal concentrations much closer to observations while was still able to reproduce reasonably the liquid phase properties although LWP=158 g m^{-2} was somewhat smaller than observed. The run IN×100 (with IN comparable with the highest values in Fridlind et al., 2007) produced IWP of 30 g m^{-2}, about 5–7 times smaller than observed.

The Prenni et al., Fridlind et al., and Morrison et al. simulations can be ranked according to sensitivity to presence of ice. The RAMS bulk model (Prenni et al., 2007) is most sensitive, full glaciation occurs at N_c~0.2 L^{-1} without depletion; the MM5 model with Morrison's microphysics is intermediate, mixed-phase can exist at N_c~1.6 L^{-1}; and the spectral bin model (Fridlind et al., 2007) allows existence of quasi-stationary mixed-phase cloud with the highest N_c~5–10 L^{-1}. A detailed comparison of 17 single column

ACPD
10, 2669–2710, 2010

models (SCM) and 9 cloud resolving models (CRM) performed in Klein et al. (2009) and Morrison et al. (2009) showed a great diversity of simulated crystal concentrations (about five orders of magnitude).

Fan et al. (2009, hereafter F09) simulated this single-layer mixed-phase cloud observed from MPACE using a 3-D model with spectral bin microphysics. The heterogeneous ice nucleation scheme chosen by F09 was more detailed than in most of the previous models: the KC scheme referred to as HIN_KC in F09. This scheme failed to reproduce the observed crystal concentrations, and F09 introduced two additional hypothetical mechanisms of ice nucleation enhancement considered in Fridlind et al. (2007): a) activation of droplet evaporation residues by condensation followed by freezing, and b) droplet evaporation freezing by contact freezing inside out.

Examination of F09 indicates that the concentration of the initial freezing aerosol particles in KC scheme was chosen incorrectly by F09. The KC scheme of DF heterogeneous nucleation assumes that freezing IN are mixed aerosol particles with concentrations comparable to cloud condensation nuclei (CCN); therefore, the aerosol concentrations for this MPACE case should have been specified to be ~72–75 cm^{-3} (~10^5 L^{-1}) in the fine mode, or ~1–2 cm^{-3} (~1–2×10^3 L^{-1}) in the coarse mode as aerosol concentration. Instead, F09 used as input IN concentration a value of N_{IN}=0.2 L^{-1} that was measured with CFDC (Prenni et al., 2007; Morrison et al., 2008). Hence F09 used values of IN concentration that were ~10^4–5×10^5 times smaller than value that should have been used in the KC scheme.

Recall that IN concentrations in chamber measurements are determined as the crystal concentration $N_{c,ch}$ at the exit of the chamber, but not as the concentration N_a of original aerosol particles at the entrance of the chamber that may potentially become ice crystals. It is known that $N_{c,ch}$ is generally 10^{-5}–10^{-3} times smaller than N_a, and it depends on conditions in the chamber. In this case, $N_{c,ch}$~ 0.2 L^{-1} measured in CFDC was two orders of magnitude smaller than measured *in situ* crystal concentrations (up to 20–30 L^{-1}). The mistake in F09 in using ice KC scheme was that the output CFDC information, already nucleated crystals in concentration of 0.2 L^{-1} (a tiny fraction of N_a)

ACPD
10, 2669–2710, 2010

was used instead of the input information, the original aerosol in concentration N_a that potentially could form crystals. The original KC scheme uses aerosol concentration N_a as input and only a very small fraction of it, 10^{-5}–10^{-3}, becomes eventually crystals (KC05).

Here we show that correct use of the KC ice scheme with the DF nucleation mode alone produces reasonable crystal concentrations in quite good agreement with the MPACE observations. The MPACE cloud is simulated using a 1-D single-column type model with spectral bin microphysics and supersaturation equation similar to described in Khvorostyanov et al. (2001, 2003) and used previously for simulation of the mixed-phase arctic clouds observed during the SHEBA-FIRE experiment (Khvorostyanov et al., 2001, 2003). The version of the model used for the MPACE simulations was modified to include the KC ice nucleation scheme and also a revised droplet nucleation scheme following a generalized power law derived in KC06, KC07 as described in Sect. 3. The aerosol measured in MPACE was approximated by the two lognormal modes, fine and coarse, as described above based on Klein et al. (2006, 2009), Morrison et al. (2008) and this bimodal aerosol was allowed to serve as both CCN and ice nuclei and participate in both nucleation processes.

The model was initialized using the initial and boundary conditions provided by Klein et al. (2006), Xie et al. (2006a, b). The cloud was initially pure liquid and the drop spectra were initialized as a 3-parameter gamma distribution with an index of 6 using observed profiles of LWC and N_d (Klein et al. 2006; see Figs. 1 and 2). Subsequently, the two kinetic equations for the droplet and crystal size distribution functions were solved at each time step Δt=0.5 s along with the supersaturation equation to calculate the evolution of the liquid and ice size spectra, each included 30 gridpoints by radius. The model has 61 vertical levels with Δz=25 m, corresponding to a vertical domain of 1.5 km. The algorithms of solution were described in detail in Khvorostyanov et al. (2001, 2003).

The baseline simulated height-time display for the MPACE cloud is shown in Fig. 7. Initially, there is a rather thick liquid layer with slightly positive water supersaturation,

ACPD
10, 2669–2710, 2010

and ice supersaturation reaches 15–18% (Fig. 7a, b). Maximum droplet concentration and liquid water content (LWC) are 90 cm^{-3} and 0.4 $g\,m^{-3}$ (Fig. 7c, e) in the upper cloud layer above 1 km. Crystals appear after 30 min of simulation, in a narrow layer near the temperature minimum (~–15 °C) at z=1.3 km with RHW~100% (Fig. 7d, f). Maximum crystal concentrations N_c are 20–30 L^{-1} in the generating layer, ice virga fall out from it, and N_c~5–10 L^{-1} in the lower layers, generating precipitation that reaches the surface.

The simulated ice nucleation has an oscillatory character (clearly seen in Fig. 7f) that results from the competition between supersaturation production by dynamical and radiative forcings and supersaturation depletion due to vapor deposition to the drops and crystals. These oscillations resemble those in the evolution of the cirrus clouds with homogeneous ice nucleation (Sassen and Dodd, 1989; Khvorostyanov et al., 2001; Sassen et al., 2002). Complete glaciation of the simulated cloud does not occur, since the crystal concentrations are too low and their supersaturation relaxation times are 1–1.5 h (Fig. 1j), the rate of vapor deposition is low, and the Bergeron-Findeisen mechanism acts slowly. Thus, a mixed-phase cloud exists and reaches a quasi-steady state with very slow gradual accumulation of ice content. The crystal concentrations of 5–15 L^{-1} do not cause full glaciation due to the large crystal relaxation time.

Figure 8 compares the simulated vertical profiles of N_d, N_c, LWC, and IWC for the MPACE case on 10 October 2006 with the observational data for 9 October. It is noted here that the large-scale flow pattern and cloud field varied little during 9–10 October (Verlinde et al., 2007; Morrison et al., 2008). The simulated droplet concentration is close to the initial profile, and maximum LWC decreased to 0.3 $g\,m^{-3}$. Simulated crystal concentration in the upper layer 0.75–1.5 km closely resembles the measured N_c: there is a pronounced maximum in N_c~30 L^{-1} at ~1.25 km, both in simulations and observations, that coincides with the temperature minimum −15 to −16.5 °C, where a substantial increase in ice nucleation rate via the DF mode is predicted the by KC theory (KC00, KC04b, KC05).

Thus, this simulation shows that the KC scheme in DF mode is capable of explaining

many features of the crystal concentrations observed during MPACE and coexistence of the liquid and ice phases. The lower maximum near 0.5 km in measured N_c is not reproduced by the simulations, and its origin is not clear. This could be a result of the nucleation due to evaporated droplet residues or droplet freezing near the lower cloud boundary as suggested in Fridlind et al. (2007).

As Figs. 7 and 8 show, correct application of the KC scheme produces quite reasonable N_c and their profiles close to observed, and that F09's conclusion that "... HIN_KC ... cannot produce the observed ice crystal concentrations without ice enhancement mechanisms" was based on an incorrect application of the KC scheme.

6 Conclusions

Some empirical parameterizations of heterogeneous ice nucleation for cloud and climate models were analyzed and compared in this work with the theoretical scheme developed by the authors (KC scheme) and based on a modification of the classical nucleation theory. The results can be briefly summarized as follows.

Analysis of several frequently used empirical parameterizations of heterogeneous ice nucleation in the context of extended classical nucleation theory indicates that most empirical parameterizations are prohibited in some ranges of their variables from the thermodynamic point of view since they correspond to negative critical radii or humidities below the critical threshold. This indicates that the existing empirical parameterizations should be corrected and those developed in the future should be constructed with account for the thermodynamic constraints. These thermodynamic limitations also should be accounted when evaluating various parameterizations in cloud models.

A detailed comparison of the empirical parameterization by Phillips et al. (2008) with the theoretical approach by Khvorostyanov and Curry (2000–2009) is performed using parcel model simulations. Both schemes are compared with climatological data on cloud phase and with its parameterization in several GCMs. This comparison demonstrated that the PDA08 scheme has a lower than required efficiency and substantially

ACPD
10, 2669–2710, 2010

underestimates crystal concentrations, while the KC scheme performs much better. PDA08 predicts almost entirely liquid cloud down to −35 °C, while KC scheme yields cloud phase much closer to climatology and GCM's parameterizations of cloud water phase.

However, some criticisms of the KC scheme expressed in PDA08 are valid. The KC scheme was developed and is applied using a single value of each input parameter, e.g. contact angle, misfit strain, etc. Therefore, the KC scheme would be improved by averaging over some ranges of the input parameters, perhaps in the way similar to Marcoli et al. (2007). Such a smoothing of the KC scheme was demonstrated in EDK09. Similar improvements are planned for the future studies.

Another evaluation of the KC scheme was performed by a comparison of the results of numerous parcel runs with KC ice nucleation scheme to the results of ice nuclei (nucleated crystals) measurements in six recent field campaigns and in some laboratory measurements. The results plotted as a function of the temperature or ice supersaturation show that the KC scheme agrees well with the experimental data on nucleated crystals concentrations.

It is demonstrated that criticism of the KC scheme by Phillips et al. (2008) of having a T-dependence of $N_c(T)$ that was too steep was caused simply by an incorrect representation of the KC scheme. The KC curve was constructed in PDA08 without any simulations, just by calculation of N_c from Eq. (8) separately for each T, and without account for the supersaturation dependence in the KC scheme that limit N_c at much smaller values.

Increasing attention is being paid to the existence and long lifetime of the mixed-phase Arctic clouds, which has been a substantial challenge for heterogeneous ice nucleation parameterizations. Numerous simulations have been conducted of a mixed phase cloud observed during the MPACE field experiment conducted near Barrow in October 2004. The common problem encountered by all models in these simulations was a very low concentration of IN measured during MPACE, ~0.16–0.2 L^{-1} on average. As a result, various hypotheses were invoked to explain occurrence of ice crys-

ACPD
10, 2669–2710, 2010

tals up to 10–30 L^{-1} in observed clouds, including activation of droplet evaporation residues, and droplet evaporation freezing.

Simulations conducted here using a single column model with spectral bin microphysics and the KC ice nucleation scheme were able to reproduce the correct quasi-steady mixed phase of this cloud for a few hours even without invoking some additional hypothetical mechanisms. We note that a previous application of the KC scheme for this case by Fan et al. (2009) incorrectly applied the parameterization by using the observed IN concentration, rather than the observed concentration of total aerosol as it should be done.

The discrepancy between the IN measured during MPACE by the CFDC instrument and the IN predicted by the KC scheme from the total aerosol concentration raises the issue of the appropriate interpretation of the IN measured by the CFDC. There are several possible reasons for not detecting these IN by the CFDC. Limitation of the aerosol diameter in CFDC by 1.5 µm while measured aerosol had a second mode near 2.6 µm, so that the largest and most effective IN could be missed in CFDC. The process of ice nucleation via freezing may take from a few minutes to a few hours, while the processing time in the CFDC is limited to 7–15 s (PDA08); thus the IN captured in CFDC could have insufficient time for ice nucleation.

Acknowledgements. The authors are grateful to Steve Klein and Renata McCoy for providing the initial data for MPACE simulations, to Jiwen Fan and Mikhail Ovtchinnikov for providing the processed aircraft data from the MPACE campaign period B, to Paul DeMott and Trude Eidhammer for providing the IN data from CFDC from 6 field campaigns, and some data of parcel model simulations with the CSU model. All of these persons are thanked for useful discussions. This research was supported by a NASA MAP grant.

References

Al-Naimi, R. and Saunders, C. P. R.: Measurements of natural deposition and condensation-freezing ice nuclei with a continuous flow chamber, Atmos. Environ., 19, 1871–1882, 1985.

Barahona, D. and Nenes, A.: Parameterization of cirrus formation in large scale models: Homogenous nucleation, J. Geophys. Res., 113, doi:10.1029/2007JD009355, 2008.

Barahona, D. and Nenes, A.: Parameterizing the competition between homogeneous and heterogeneous freezing in cirrus cloud formation – monodisperse ice nuclei, Atmos. Chem. Phys., 9, 369–381, 2009, http://www.atmos-chem-phys.net/9/369/2009/.

Berezinsky, N. A. and Stepanov, G. V.: Dependence of natural ice-forming nuclei concentration of different size on the temperature and supersaturation, Izv. Acad. Sci. USSR, Atmos. Oceanic Phys., 22, 722–727, 1986.

Bigg, E. K.: The formation of atmospheric ice crystals by the freezing of droplets, Q. J. Roy. Meteor. Soc., 79, 510–519, 1953.

Borovikov, A. M., Gaivoronsky, I. I., Zak, E. G. et al.: Cloud Physics, Leningrad, Hydrometeoizdat, 1961, Transl. by Israel Program Scientif. Translation, US Department of Commerce, Washington, DC, 459 pp., 1963.

Boville, B. A., Rasch, P. J., Hack, J. J., and McCaa, J. R.: Representation of clouds and precipitation processes in the Community Atmosphere Model version 3 (CAM3), J. Climate, 19, 2184–2198, 2006.

Chen, J.-P., Hazra, A., and Levin, Z.: Parameterizing ice nucleation rates using contact angle and activation energy derived from laboratory data, Atmos. Chem. Phys., 8, 7431–7449, 2008, http://www.atmos-chem-phys.net/8/7431/2008/.

Comstock, J. M., Lin, R.-F., Starr, D. O'C., and Yang, P.: Understanding ice supersaturation, particle growth, and number concentration in cirrus clouds, J. Geophys. Res., 113, D23211, doi:10.1029/2008JD010332, 2008.

Cooper, W. A.: Ice initiation in natural clouds. Precipitation Enhancement. A Scientific Challenge, Meteor. Mon., 21, p. 28, 1986.

Cotton, W. R. and Anthes, R. A.: Storm and Cloud Dynamics, Academic Press, NY, USA, 883 pp., 1989.

Cotton, W. R., Pielke Sr., Walko, R. A. R. L., Liston, G. E., Tremback, C. J., Jiang, H., McAnelly, R. L., Harrington, J. Y., Nicholls, M. E., Carrio, G. G., and McFadden J. P.: RAMS 2001: current status and future directions, Meteorol. Atmos. Phys., 82, 5–29, 2003.

Curry, J. A.: Interactions among turbulence, radiation and microphysics in Arctic stratus clouds, J. Atmos. Sci., 43, 525–538, 1986.
Curry, J. A., Meyer, F. G., Radke, L. F., Brock, C. A., and Ebert, E. E.: Occurrence and characteristics of lower tropospheric ice crystals in the Arctic, Int. J. Climatol., 10, 749–764, 1990.
Curry, J. A., Schramm, J., and Ebert, E. E.: Impact of clouds on the surface radiation budget of the Arctic Ocean, Meteorol. Atmos. Phys., 51, 197–217, 1993.
Curry, J. A., Rossow, W. B., Randall, D., and Schramm, J. L.: Overview of Arctic cloud and radiation properties, J. Climate, 9, 1731–1764, 1996.
Curry, J. A., Hobbs, P., King, M., Randall, D., Minnis, P. et al.: FIRE Arctic clouds experiment, B. Am. Meteorol. Soc., 81, 5–29, 2000.
Dash, J. G., Fu, H., and Wettlaufer, J. S.: The premelting of ice and its environmental consequences, Rep. Progr. Phys., 58, 115–167, 1995.
DeMott, P. J., Rogers, D. C., Kreidenweis, S. M., Chen, Y., Twohy, C. H., Baumgardner, D., Heymsfield, A. J., and Chan, K. R.: The role of heterogeneous freezing nucleation in upper tropospheric clouds: inferences from SUCCESS, Geophys. Res. Lett., 25, 1387–1390, 1998.
DeMott, P. J., Prenni, A. J., Liu, X., Kreidenweis, S. M., Petters, M. D., Twohy, C H., Richardson, M. S., Eidhammer, T., and Rogers, D. C.: Predicting global atmospheric ice nuclei distributions and their impacts on climate, Proc. Natl. Acad. Sci., submitted, 2010.
Diehl, K. and Wurzler, S.: Heterogeneous drop freezing in the immersion mode: model calculations considering soluble and insoluble particles in drops, J. Atmos. Sci., 61, 2063–2072, 2004.
Dufour, L. and Defay, R.: Thermodynamics of Clouds, Academic Press, New York, 1963.
ECMWF-2007: European Centre for Medium Range Weather Forecast (ECMWF), 2007, IFS documentation cycle 31rl, Part IV: physical processes, 155 pp., http://www.ecmwf.int/research/ifsdocs/CY31rl/index.html, last access: 17 November 2009, 2007.
Eidhammer, T., DeMott, P. J., and Kreidenweis, S. M.: A comparison of heterogeneous ice nucleation parameterization using a parcel model framework, J. Geophys. Res., 114, D06202, doi:10.1029/2008JD011095, 2009.
Fan, J., Ovtchinnikov, M., Comstock, J. M., McFarlane, S. A., and Khain, A.: Ice formation in Arctic mixed-phase clouds: insights from a 3-D cloud-resolving model with size-resolved aerosol and cloud microphysics, J. Geophys. Res., 114, D04205, doi:10.1029/2008JD010782, 2009.

Fletcher, N. H.: The Physics of Rainclouds, Cambridge University Press, Cambridge, UK, 390 pp., 1962.
Fletcher, N. H.: Active sites and ice crystal nucleation, J. Atmos. Sci., 26(6), 1266–1278, 1969.
Fridlind, A. M., Ackerman, A. S., McFarquhar, G., Zhang, G., Poellot, M. R., DeMott, P. J., Prenni, A. J., and Heymsfield, A. J.: Ice properties of single-layer stratocumulus during the Mixed-Phase Arctic Cloud Experiment: 2. Model results, J. Geophys. Res., 112, D24202, doi:10.1029/2007JD008646, 2007.
Gettelman, A., Morrison, H., and Ghan, S. J.: A new two-moment bulk stratiform cloud microphysics scheme in the Community Atmosphere Model, Version 3 (CAM3). Part II: single-column and global results, J. Climate, 21, 3660–3679, 2008.
Gierens, K.: On the transition between heterogeneous and homogeneous freezing, Atmos. Chem. Phys., 3, 437–446, 2003, http://www.atmos-chem-phys.net/3/437/2003/.
Gultepe, I., Isaac, G., Judak, D., Nissen, R., and Strapp, J. W.: Dynamical and microphysical characteristics of Arctic clouds during BASE, J. Climate, 13, 1225–1254, 2000.
Heymsfield, A. J. and Sabin, R. M.: Cirrus crystal nucleation by homogeneous freezing of solution droplets, J. Atmos. Sci., 46, 2252–2264, 1989.
Hobbs, P. V.: Ice Physics, Clarendon Press, Oxford, 837 pp., 1974.
Huffman, P. J.: Supersaturation spectra of AgI and natural ice nuclei, J. Appl. Meteorol., 12, 1080–1082, 1973.
Huffman, P. J. and Vali, G.: The effect of vapor depletion on ice nucleus measurements with membrane filter, J. Appl. Meteorol., 12, 1018–1024, 1973.
Intrieri, J. M., M Shupe, D., Uttal, T., and McCarty, B. J.: Arctic cloud statistics from radar and lidar at SHEBA, J. Geophys. Res., 107, 8030–8039, 2002.
Kärcher, B. and Lohmann, U.: A parameterization of cirrus cloud formation: heterogeneous freezing, J. Geophys. Res., 108 (D14), 4402, doi:10.1029/2002JD003220, 2003.
Khvorostyanov, V. I. and Curry, J. A.: A new theory of heterogeneous nucleation for application in cloud and climate models, Geophys. Res. Lett., 27, 4081–4084, 2000.
Khvorostyanov, V. I. and Curry, J. A.: Thermodynamic theory of freezing and melting of water and aqueous solutions, J. Phys. Chem. A, 108(50), 11073–11085, 2004a.
Khvorostyanov, V. I. and Curry, J. A.: The theory of ice nucleation by heterogeneous freezing of deliquescent mixed CCN. Part 1: critical radius, energy and nucleation rate, J. Atmos. Sci., 61(22), 2676–2691, 2004b.
Khvorostyanov, V. I. and Curry, J. A.: The theory of ice nucleation by heterogeneous freezing

of deliquescent mixed CCN. Part 2: parcel model simulation, J. Atmos. Sci., 62(2), 261–285, 2005.

Khvorostyanov, V. I. and Curry, J. A.: Aerosol size spectra and CCN activity spectra: reconciling the lognormal, algebraic, and power laws, J. Geophys. Res., 111, D12202, doi:10.1029/2005JD006532, 2006.

Khvorostyanov, V. I. and Curry, J. A.: Refinements to the Köhler's theory of aerosol equilibrium radii, size spectra, and droplet activation: effects of humidity and insoluble fraction, J. Geophys. Res., 112, D5, D05206, doi:10.1029/2006JD007672, 2007.

Khvorostyanov, V. I. and Curry, J. A.: Kinetics of cloud drop formation and its parameterization for cloud and climate Models, J. Atmos. Sci., 65, 2784–2802, 2008.

Khvorostyanov, V. I. and Curry, J. A.: Critical humidities of homogeneous and heterogeneous ice nucleation: inferences from extended classical nucleation theory, J. Geophys. Res., 114, D04207, doi:10.1029/2008JD011197, 2009a.

Khvorostyanov, V. I. and Curry:, J. A., Parameterization of cloud drop activation based on analytical asymptotic solutions to the supersaturation equation, J. Atmos. Sci., 66(7), 1905–1925, 2009b.

Khvorostyanov, V. and Sassen, K.: Towards the theory of homogeneous nucleation and its parameterization for cloud models, Geophys. Res. Lett., 25(16), 3155–3158, 1998.

Khvorostyanov, V. I., Curry, J. A., Pinto, J. O., Shupe, M., Baker, B., and Sassen, K.: Modeling with explicit spectral water and ice microphysics of a two-layer cloud system of altostratus and cirrus observed during the FIRE Arctic Clouds Experiment, J. Geophys. Res. (Special Issue), 106, 15099–15112, 2001.

Khvorostyanov, V. I., Curry, J. A., Gultepe, I., and Strawbridge, K.: A springtime cloud over the Beaufort Sea polynya: three-dimensional simulation with explicit spectral microphysics and comparison with observations, J. Geophys. Res., 108(D9), 4296, doi:10.1029/2001JD001489, 2003.

Klein, S., Fridlind, A., McCoy, R. B., McFarquhar, G., and Menon, S. et al.: GCSS Polar Cloud WG SCM/CRM/LES Intercomparison Case 2004, ARM Mixed-Phase Arctic Cloud Experiment (M-PACE): 5–22 October 2004, http://science.arm.gov/wg/cpm/scm/scmic5/, last access: 15 December 2009, 2006.

Klein, S. A., McCoy, R. B., Morrison, H. et al.: Intercomparison of model simulations of mixed-phase clouds observed during the ARM Mixed-Phase Arctic Cloud Experiment. I. Single-layer cloud, Q. J. Roy. Meteor. Soc., 135, 979–1002, 2009.

Korolev, A., Isaac, G., Cober, S. G., Strapp, J. W., and Hallett, J.: Microphysical characterization of mixed-phase clouds, Q. J. Roy. Meteor. Soc., 129, 19–38, 2003.
Lawson, R. P., Baker, B. A., Schmitt, C. G., and Jensen, T. L.: Overview of microphysical properties of summertime boundary layer clouds observed during FIRE.ACE, J. Geophys. Res., 106, 14989–15014, 2001.
Lin, R.-F., Starr, D. O'C., DeMott, P. J., Cotton, R., Sassen, K., Jensen, E., Kärcher, B., and Liu, X.: Cirrus parcel model comparison project. Phase 1: the critical components to simulate cirrus initiation explicitly, J. Atmos. Sci., 59, 2305–2329, 2002.
Liu, X. and Penner, J.: Ice nucleation parameterization for global models, Meteorol. Z., 14, 499–514, 2005.
Liu, X., Penner, J. E., Ghan, S. J., and Wang, M.: Inclusion of ice microphysics in the NCAR Community Atmospheric Model version 3 (CAM3), J. Climate, 20, 4526–4547, 2007.
Lohmann, U. and Diehl, K.: Sensitivity studies of the importance of dust ice nuclei for the indirect aerosol effect on stratiform mixed-phase clouds, J. Atmos. Sci., 63, 968–982, 2006.
Marcolli, C., Gedamke, S., Peter, T., and Zobrist, B.: Efficiency of immersion mode ice nucleation on surrogates of mineral dust, Atmos. Chem. Phys., 7, 5081–5091, 2007, http://www.atmos-chem-phys.net/7/5081/2007/.
Meyers, M. P., DeMott, P. J., and Cotton, W. R.: New primary ice-nucleation parameterizations in an explicit cloud model, J. Appl. Meteorol., 31, 708–721, 1992.
Möhler, O., Field, P. R., Connolly, P., Benz, S., Saathoff, H., Schnaiter, M., Wagner, R., Cotton, R., Krämer, M., Mangold, A., and Heymsfield, A. J.: Efficiency of the deposition mode ice nucleation on mineral dust particles, Atmos. Chem. Phys., 6, 3007–3021, 2006, http://www.atmos-chem-phys.net/6/3007/2006/.
Morrison, H. and Gettelman, A.: A new two-moment bulk stratiform cloud microphysics scheme in the community atmosphere model, Version 3 (CAM3). Part I: description and numerical tests, J. Climate, 21, 3642–3659, 2008.
Morrison, H. and Pinto, J. O.: Mesoscale modeling of springtime arctic mixed-phase stratiform clouds using a new two-moment bulk microphysics scheme, J. Atmos. Sci., 62, 3683–3704, 2005.
Morrison, H., Curry, J. A., and Khvorostyanov, V. I.: A new double-moment microphysics parameterization. Part 1: description, J. Atmos. Sci., 62, 1665–1674, 2005.
Morrison, H., Pinto, J. O., Curry, J. A., and McFarquhar, G. M.: Sensitivity of modeled arctic mixed-phase stratocumulus to cloud condensation and ice nuclei over regionally varying

surface conditions, J. Geophys. Res., 113, D05203, doi:10.1029/2007JD009729, 2008.
Morrison, H., McCoy, R. B., Klein, S. A. et al.: Intercomparison of model simulations of mixed-phase clouds observed during the ARM Mixed-Phase Arctic Cloud Experiment. II. Multilayer cloud, Q. J. Roy. Meteor. Soc., 135, 1003–1019, 2009.
Philips, V. T. J., DeMott, P. J., and Andronache, C.: An empirical parameterization of heterogeneous ice nucleation for multiple chemical species of aerosol, J. Atmos. Sci., 65, 2757–2783, 2008.
Prenni, A. J., Harrington, J. Y., Tjernström, M., DeMott, P. J., Avramov, A., Long, C. N., Kreidenweis, S. M., Olsson, P. Q., and Verlinde, J.: Can ice-nucleating aerosols affect Arctic seasonal climate?, B. Am. Meteorol. Soc., 88(4), 541–550, 2007.
Pruppacher, H. R. and Klett, J. D.: Microphysics of Clouds and Precipitation, 2nd Edn., Kluwer, Dordrecht, The Netherlands, 997 pp., 1997.
Rogers, D. C.: Field and laboratory studies of ice nucleation in winter orographic clouds, Ph. D. dissertation, Department of Atmospheric Science, University of Wyoming, Laramie, 161 pp., 1982.
Rogers, D. C.: Development of a continuous flow thermal gradient diffusion chamber for ice nucleation studies, Atmos. Res., 22, 149–181, 1988.
Sassen, K.: Ice nuclei availability in the higher tropospheric: implications od a remote sensing cloud phase climatology, in: Nucleation and Atmospheric aerosols, edited by: Fukuta , N. and Wagner, P., Deepak Publishing, Hampton, Virginia, USA, 287–290, 1992.
Sassen, K. and Dodd, G. C.: Homogeneous nucleation rate for highly supercooled cirrus cloud droplets, J. Atmos. Sci., 45, 1357–1369, 1988.
Sassen, K. and Dodd, G. C.: Haze particle nucleation simulation in cirrus clouds, and application for numerical and lidar studies, J. Atmos. Sci., 46, 3005–3014, 1989.
Sassen, K. and Benson, S.: Ice nucleation in cirrus clouds. A model study of the homogeneous and heterogeneous nucleation modes, Geophys. Res. Lett., 27, 521–524, 2000.
Sassen, K., Wang, Z., Khvorostyanov, V. I., Stephens, G. L., and Bennedetti, A.: Cirrus cloud ice water content radar algorithm evaluation using an explicit cloud microphysical model, J. Appl. Meteorol., 41, 620–628, 2002.
Seinfeld, J. H., and Pandis, S. N.: Atmospheric Chemistry and Physics, Wiley, New York, 1326 pp., 1998.
Shupe, M. D., Matrosov, S. Y., and Uttal, T.: Arctic mixed-phase cloud properties derived from surface-based sensors at SHEBA, J. Atmos. Sci., 63, 697–711, 2006.

Thomson, J. J.: Application of Dynamics to Physics and Chemistry, 1st Edn., Cambridge University Press, London, UK, 163 pp., 1888.
Vali, G.: Nucleation terminology, J. Aerosol. Sci., 16, 575–576, 1985.
Vehkamäki, H., Määttänen, A., Lauri, A., Napari, I., and Kulmala, M.: Technical Note: The heterogeneous Zeldovich factor, Atmos. Chem. Phys., 7, 309–313, 2007, http://www.atmos-chem-phys.net/7/309/2007/.
Verlinde, J., Harrington, J. Y., McFarquhar, G. M., Yannuzzi, V. T., Avramov, A., et al.: Overview of the Mixed-Phase Arctic Cloud Experiment (MPACE), B. Am. Meteorol. Soc., 88, 205–201, 2007.
Xie, S., Klein, S. A., Yio, J. J., Beljaars, A. C. M., Long, C. N., and Zhang, M.: An assessment of ECMWF analyses and model forecasts over the North Slope of Alaska using observations from the ARM Mixed-Phase Arctic Cloud Experiment, J. Geophys. Res., 111, D05107, doi:10.1029/2005JD006509, 2006a.
Xie, S., Klein, S. A., Zhang, M., Yio, J. J., Cederwall, R. T., and McCoy, R.: Developing large-scale forcing data for single-column and cloud-resolving models from the Mixed-Phase Arctic Cloud Experiment, J. Geophys. Res., 111, D19104, doi:10.1029/2005JD006950, 2006b.
Young, K.: Microphysical Processes in Clouds, Oxford University Press, New York, USA, 427 pp., 1993.
Yum, S. S. and Hudson, J. G.: Vertical distributions of cloud condensation nuclei spectra over the springtime Arctic Ocean, J. Geophys. Res., 106(D14), 15045–15052, 2001.
Zeldovich, J. B.: Toward the theory of formation of a new phase. Cavitation, J. Exp. Theor. Phys., 12, 525, 1942.

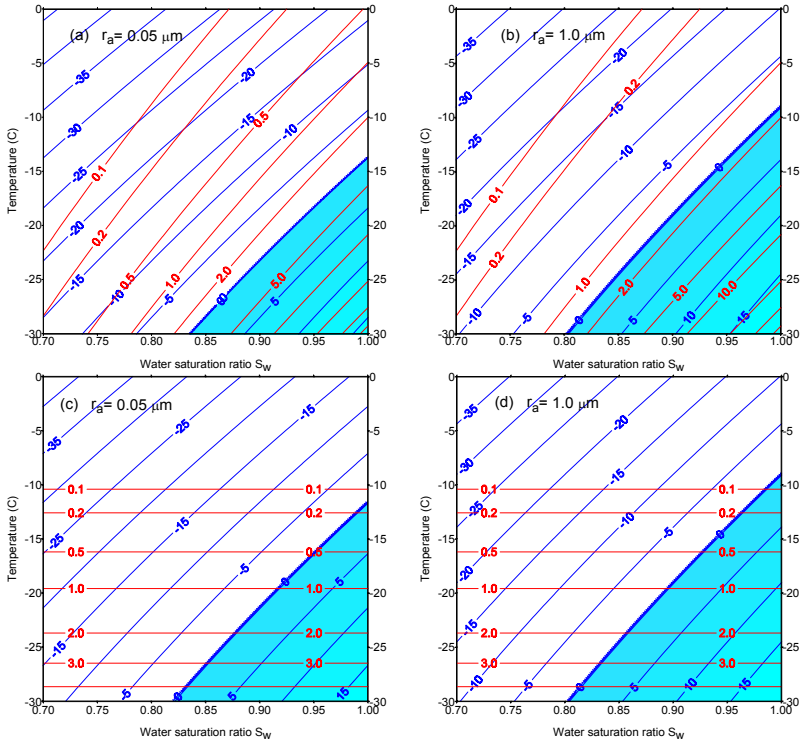

Fig. 1. S_w–T diagrams of N_c calculated with MDC92 **(a, b)** and DM10 **(c, d)** parameterizations (red lines and labels) with superimposed threshold difference $\delta(\mathrm{RHW_{th}}) = \mathrm{RHW}-\mathrm{RHW_{th}}=(S_w-S_{w,th})\times 100\%$ (blue lines and labels) calculated as in KC09. The line $\delta(\mathrm{RHW_{th}})=0$ or $\mathrm{RHW}=\mathrm{RHW_{th}}$ is indicated by deep blue and hatched. The physical states and N_c above this line (white field) are below the critical humidity, $S_i<S_{i,cr}$, are thermodynamically prohibited, and correspond to the negative critical radii, $r_{cr}<0$. Only the states below the blue hatched line $\mathrm{RHW}-\mathrm{RHW_{th}}=0$ (blue shaded field) are thermodynamically allowed. They correspond to $r_{cr}>0$, but N_c in these domains do not correspond to N_c calculated from the classical nucleation theory.

ACPD
10, 2669–2710, 2010

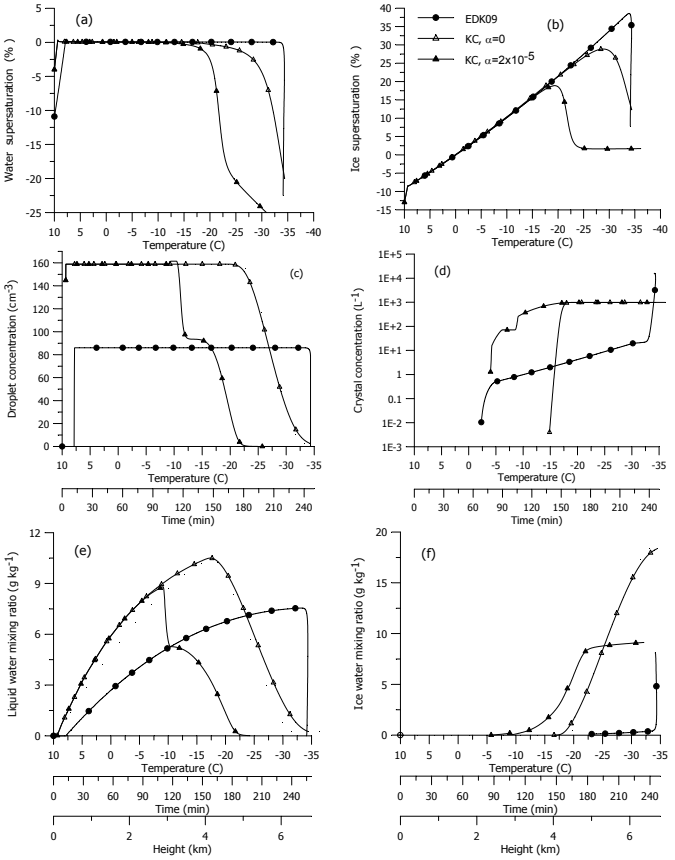

Fig. 2. Comparison of the temperature and time dependencies of cloud microphysical properties in the parcel runs obtained in simulations EDK09 with parameterization PDA08 (solid circles) and obtained in simulations of this work using KC scheme with DF mode and two models of active sites: α=0 (open triangles) and $\alpha(T)$ as a linear function of T (solid triangles) as described in the text. The parameters of the runs: w=50 cm s^{-1}, RHW$_0$=89%, N_a = 200 cm^{-3}.

ACPD
10, 2669–2710, 2010

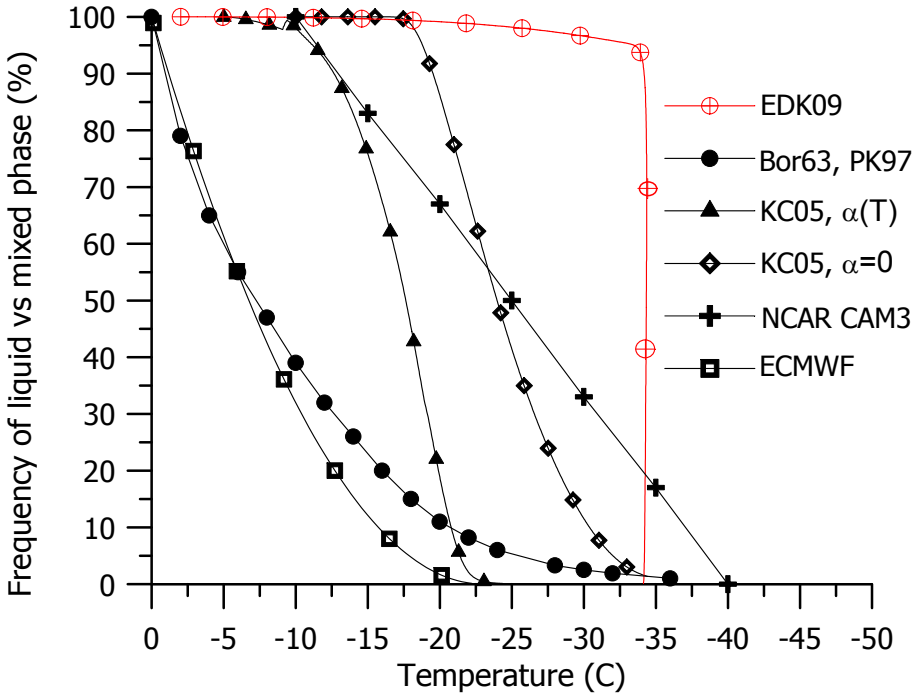

Fig. 3. Frequency of liquid vs. mixed states. Climatological data after Borovikov et al. (1963) (see also Fig. 2-33 in PK97), compared to the characteristic of the liquid/mixed phase, the ratio f_l=LWC/(LWC+IWC), simulated with the KC05 and parcel model and heterogeneous KC ice scheme with only 2nd aerosol mode included, N_{d2}=1 cm^{-3}, σ_{d2}=2, r_{d2}=0.4 μm, and 2 values of active site areas: α=0 (diamonds), and $\alpha(T)$ as described in the text (triangles), and simulated in EDK09 parcel model with PDA08 ice scheme with the same aerosol and α=0 (open circles). These simulations are compared to the corresponding T-partitioning of the liquid and ice phases in the climate models with single-moment microphysics: the NCAR CAM3 (Boville et al., 2006), (83% liquid at −15°C) and ECMWF (ECMWF-2007), (12% liquid at −15°C) as described in the text.

ACPD
10, 2669–2710, 2010

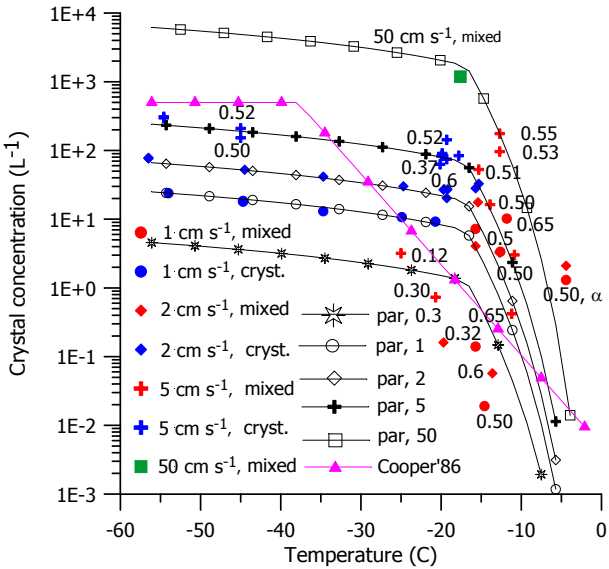

Fig. 4. Temperature dependence of the crystal concentrations N_c calculated with w=1 (solid circles), 2 (diamonds), and 5 cm s^{-1} (crosses), and 50 cm s^{-1} (green square). Each solid symbol corresponds to a final N_c after a single run of the parcel model with KC (2000, 2004, 2005) heterogeneous DF ice nucleation scheme. The values of the contact parameter m_{is}=0.52=const along the continuous lines, the other values of m_{is} are shown near the points that are outside the lines; the symbol "α" denotes the runs with $\alpha=2\times10^{-5}$. Red symbols denote CCN freezing at $\delta_w>0$ in the presence of drops in a mixed cloud, mostly at $T_c>-20$ °C, although mixed phase can be below −20°C and down to −30 °C with lower m_{is}=0.12–0.30. Blue symbols denote ice nucleation at $\delta_w<0$ in a crystalline cloud. The solid lines with the open symbols plotted for w=0.3, 1, 2, 3, 5, and 50 cm s^{-1} are parameterizations from KC05 of the simulation data as described in the text. These lines are compared with Cooper's (1986) parameterization (triangles). These fits might be used as a simple parameterization of the average data in figure in cloud models and GCMs.

ACPD
10, 2669–2710, 2010

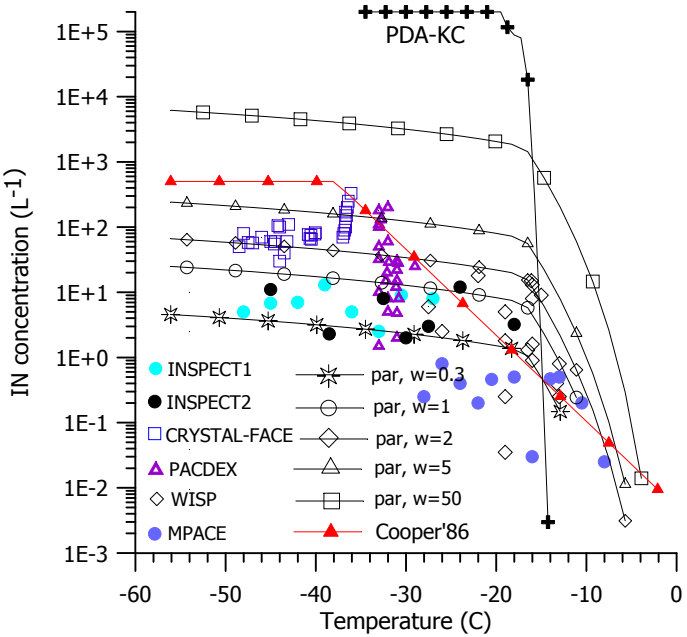

Fig. 5. Parameterized parcel model simulations from KC scheme with DF mode shown in Fig. 4 for the 5 values of w=0.3, 1, 2, 5 and 50 cm s^{-1} are compared to the experimental data from the 6 field campaigns described in Eidhammer et al. (2009) and indicated in the legend. The almost vertical curve labeled "PDA-KC" is from Philips et al. (2008). This curve, labeled "KC" in PDA08, was calculated from Eq. (8) for N_c here at S_w=1 (RHW=100%) for each T separately, without any model simulations and was a wrong attempt to represent the T-dependence in KC theory with excluded S_w-dependence and its negative feedback. As this figure illustrates, this curve is substantially different from the real T-dependences in KC scheme represented by the parameterized KC curves. This PDA-KC curve from PDA08 actually represents the old T-dependence from the classical theory based on the J. J. Thomson's (1888) Eqs. for r_{cr} and ΔF_{cr} with account for only T-dependence but without S_w-dependence (see PK97, Eq. 9–38).

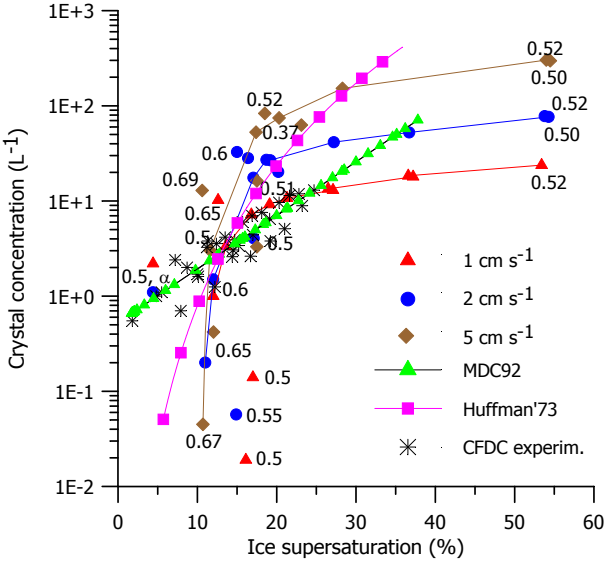

Fig. 6. The ice supersaturation dependence of the crystal concentration $N_c(s_i)$ calculated with KC04-KC05 scheme. Each solid circle on the curves corresponds to a final N_c after a single run of the parcel model with α=0. The data are mostly the same as in Fig. 4 but plotted here as a function of ice supersaturation. The red, blue and brown symbols and lines denote simulations with vertical velocity w=1, 2 and 5 cm s^{-1}. The contact parameter m_{is}=0.52 along the lines (as shown at the right ends) and is indicated near the points where it is different from 0.52; the symbol "α" denotes the runs with active site parameter $\alpha=2\times10^{-5}$, which yields N_c=1–3 L^{-1} at $s_i\approx5\%$. With this or similar value α, all points would be shifted to lower supersaturations by ~5–7% and would be closer to MDC92 curve and experimental points at lower ice supersaturations. The parameterization curve from Meyers et al. (MDC92, extended to s_i=38%) is denoted with green color and triangles. Huffman's (1973) parameterization $N_c(s_i)=C_{iH}s_i^b$ with $C_{iH}=10^{-5}$ L^{-1} (chosen here to match the lab data) and b=4.9 is shown in magenta. Black crosses denote experimental points from CFD chamber by Rogers (1982, 1988) and Al-Naimi and Saunders (1985) (courtesy by Paul DeMott).

ACPD
10, 2669–2710, 2010

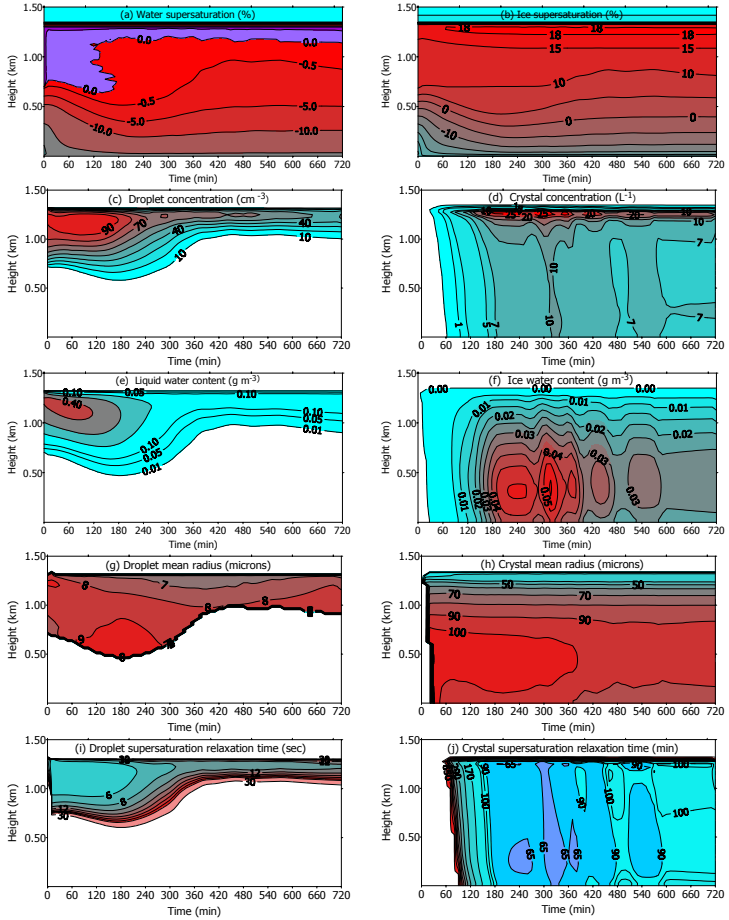

Fig. 7. Evolution of the Arctic mixed-cloud microphysical properties over 12 h with initial M-PACE data on 10 October 2004, KC04-05 ice scheme (condensation-freezing mode only) and KC06-07 drop activation scheme.

ACPD
10, 2669–2710, 2010

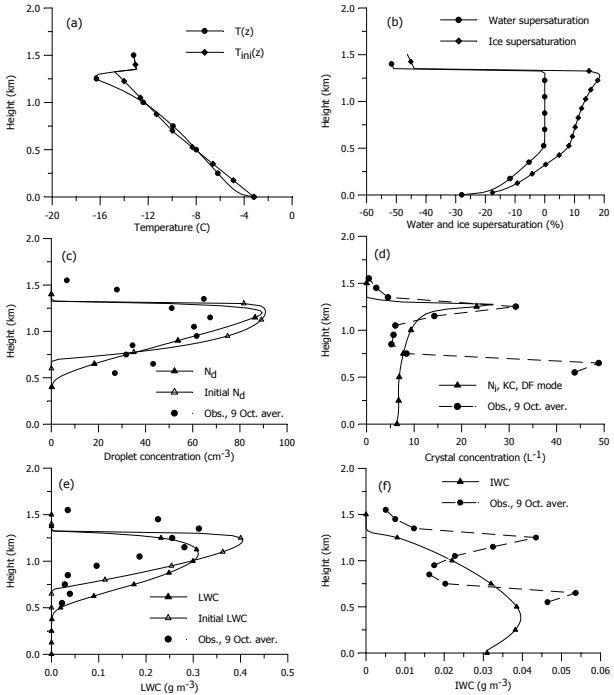

Fig. 8. Vertical profiles of N_d, N_i, LWC, and IWC for simulations of MPACE on 10 October 2006, corresponding to the time t=3 h in cross-sections in Fig. 7, compared to the observational data for 9 October. KC ice nucleation scheme was used with account for deliquescence-freezing (DF) mode, and KC06-07 CCN activation scheme was used for drop nucleation. All aerosol with 2 observed lognormal modes (N_{a1}=72.2 cm^{-3}, r_m=0.052 µm, σ=2.04; N_{a2}=1.8 cm^{-3}, r_m=1.3 µm, σ=2.5) was allowed to serve as both CCN and ice nuclei and participate in both nucleation processes. Note a pronounced maximum in N_i at ~1.25 km, both in simulations and observations, that coincides with the temperature minimum −16 to −16.5 °C, where a substantial increase in ice nucleation rate is predicted by KC theory (KC04, KC05).

ACPD
10, 2669–2710, 2010